CHALMERS
UNIVERSITY OF TECHNOLOGY

An Accurate Analytical Method for Leakage Inductance Calculation of Shell-Type Transformers With Rectangular Windings

Citation for the original published paper (version of record):
Eslamian, M., Kharezy, M., Thiringer, T. (2021). An Accurate Analytical Method for Leakage Inductance Calculation of Shell-Type Transformers
With Rectangular Windings. IEEE Access, 9: 72647-72660.
http://dx.doi.org/10.1109/ACCESS.2021.3080242

(article starts on next page)

IEEE Access
Multidisciplinary | Rapid Review | Open Access Journal

Received April 29, 2021, accepted May 10, 2021, date of publication May 13, 2021, date of current version May 21, 2021.

Digital Object Identifier 10.1109/ACCESS.2021.3080242

An Accurate Analytical Method for Leakage Inductance Calculation of Shell-Type Transformers With Rectangular Windings

MORTEZA ESLAMIAN[1], MOHAMMAD KHAREZY[2], (Member, IEEE), AND TORBJÖRN THIRINGER[3], (Senior Member, IEEE)

[1]Department of Electrical Engineering, University of Zanjan, Zanjan 45371-38791, Iran
[2]Department of High Voltage Measurement Technology, Research Institutes of Sweden (RISE), 504 62 Borås, Sweden
[3]Department of Electrical Engineering, Chalmers University of Technology, 412 96 Gothenburg, Sweden

Corresponding author: Morteza Eslamian (eslamian@znu.ac.ir)

This work was supported in part by the Swedish Energy Agency under Grant 44983-1, in part by the ÅForsk under Grant 15-566, and in part by the Research Institutes of Sweden (RISE).

ABSTRACT This paper presents an accurate analytical method for calculating the leakage inductance of shell-type E-core transformers with rectangular windings. For this purpose, first, an expression for calculating the leakage inductance per unit length inside the core window considering the core walls as the flux-normal boundary condition is derived. Then, a new accurate method for determining the Mean Length of Turns (MLT) based on the total stored energy is presented. The MLT is needed for the leakage inductance calculation using 2-D methods. By dividing the MLT into three partial lengths and calculating the corresponding leakage inductances using three different core window arrangements, the effect of core structure on the total leakage inductance is considered. The method is verified by 3-D FEM simulations as well as the leakage inductance measurements on two different fabricated transformer prototypes. The superiority of the method is also confirmed by comparisons with the previous analytical approaches. The proposed method enables the leakage inductance calculation with an error less than 1%, compared to the 3-D FEM results. Using the presented method, the leakage inductance calculations can be performed rapidly and accurately in the design stage without the need for time-consuming 3-D FEM simulations.

INDEX TERMS Leakage inductance, shell-type transformer, MFT.

I. INTRODUCTION

One of the popular types of the high-power DC-DC converters is the Dual Active Bridge (DAB) converter with application areas like smart grids and highly restricted applications such as traction and offshore wind farms [1], [2]. A DAB converter is shown in Fig. 1. The converter benefits from a Medium Frequency Transformer (MFT) to transfer the power between the primary and secondary bridges and this results in a high-power density unit. The MFT is subjected to square voltage waveforms from both sides. Such a transformer serves as an inductance, in addition to its natural duty of galvanic isolation between the primary and secondary bridges. For achieving a soft switching operation, a minimum series inductance is required to be integrated with the leakage inductance of the MFT [3]. An insufficient leakage inductance can adversely affect the converter efficiency while higher values of leakage inductance can cause an unnecessary reactive power circulation within the converter [4]. Therefore, the design of an MFT should fulfill the criteria of having a determined leakage inductance in addition to meet the other design requirements such as the specified isolation, efficiency and the thermal requirements [3], [5], [6], [7].

In recent works [4], [8]–[10] the effect of frequency on the leakage inductance of high frequency transformers (HFT) has been studied up to 2 MHz using the Dowell method [11] or its improved form [12]. In order to reduce the frequency-dependent eddy current losses of the windings, Litz wire is generally used in medium frequency transformers. It contains a large number of conductor strands with a small diameter of for example 0.1 or 0.2 mm. Since the skin depth is greater than the diameter of conductor, the change in

The associate editor coordinating the review of this manuscript and approving it for publication was Yilun Shang.

current distribution and consequently the leakage inductance variation with respect to frequency is negligible at least up to 20 kHz which is a relatively high value as the rated frequency of an actual MFT [13]–[15].

Several methods for calculation of the leakage inductance of a transformer can be found in the literature. In the classical method, the effect of the core is neglected, and it is also difficult to consider asymmetries in distributions of Ampere-turns. The effect of the radial component of flux on the leakage inductance is considered by applying the Rogowski factor to the average height of the windings [16], [17]. In [18], unbalanced ampere-turn due to the different heights of windings is treated with the linear superposition of the longitudinal and transverse magnetic fields to avoid large errors of the classical analytical model.

A popular approach to calculate axial and radial components of the leakage field taking the effect of the iron core into account is the method of images [19], [20]. The calculation of the leakage inductance of toroidal transformers based on the analytical integration of the stored energy is presented in [21].

A method based on double Fourier series, originally proposed by Roth [22], was developed in [23] to calculate the leakage reactance for an arbitrary arrangement of windings. In this method, the core window is considered as π radians wide and π radians long, regardless of its absolute dimensions. The magnetic field analysis of rectangular conductors in a closed slot using double Fourier series was extended in [24]. By simplifying the infinite sums obtained for the vector potential, a closed-form relation was proposed for the leakage inductance of a two-winding transformer. Based on the application of Roth's method, the influence of various factors (such as axial or radial cooling ducts) on the leakage inductance of transformers was investigated in [25]. The advantages and the limitations of the Roth's method are discussed in [26] from the mathematical point of view. In [27], different analytical methods used for calculation of the leakage inductance are compared with respect to the accuracy and computation time.

The application of the finite element method (FEM) for calculation of the leakage inductance has been the subject of study for decades [28]–[30]. The main advantage of FEM is that it can be employed to complex geometries. The FEM analysis is very accurate; however, it requires much longer time to execute compared with the analytical methods especially during the design stage. Moreover, a FEM tool or a special finite element analysis program is also needed for this purpose.

For calculating the leakage inductance of shell-type transformers with rectangular windings using the conventional method, first, the inductance per unit length is calculated by a 1-D or 2-D field analysis and then by multiplying the inductance per unit length by the mean length of turns (MLT) the total leakage inductance is obtained [27], [31]. There is no definitive method for determining the MLT in the literature. In a shell-type transformer, the energy stored in the corner regions of the rectangular windings has a significant effect on the leakage inductance, which has not been dealt with enough in the previous analytical methods. Missing in available literature is thus an accurate method for determining the MLT. Furthermore, an important issue is to incorporate the effect of the boundary conditions caused by the core walls in the leakage inductance calculation which is less considered in the previous studies.

In a previous work of the authors [32], an analytical method for calculating the leakage inductance of MFTs with rectangular windings was presented. The inductances per unit length, denoted by L_{in} and L_{out}, are calculated using a 2-D field analysis inside and outside the core window. The MLT is equal to the perimeter of a hypothetical rectangle whose sides are located in the middle of the total width of the windings and the main gap on each side. Based on the part of the MLT which is surrounded by the core, the MLT is divided in two partial lengths MLT_{in} and MLT_{out}. The total leakage inductance is then obtained by the summation of $MLT_{in}L_{in}+MLT_{out}L_{out}$. Good results were observed for this method compared to the measurement results. However, further research done by the authors shows that the proposed method is not general enough and by changing the dimensions of the windings or the core, the accuracy of leakage inductance may decrease. The results of multiple 3-D FEM simulations performed in the current work show that despite the considerations made in calculating the leakage inductance per unit length, determination of the MLT in the usual way is not accurate enough, resulting to errors in the total leakage inductance.

In this paper, first, an analytical method based on a two-dimensional field analysis is provided in Section II for calculation of the leakage inductance inside the core window. The proposed method can be considered as a reformulation of Roth's method for the problem of calculating the leakage inductance inside a closed slot. By applying the double Fourier series to the governing equation and considering the boundary conditions defined on the core walls, the vector potential relation for each coil is obtained in the form of infinite double series. Having the vector potential relation, the leakage inductance per unit length is obtained for any arbitrary arrangement of coils inside the core window. As the next step, in Section III, a new method for determination of the MLT based on the total energy stored in the axial leakage field is presented. In this method, the effect of the distribution of Ampere-turns in individual layers of the windings is considered in determining the MLT. Considering the boundary conditions exerted by the core walls, the MLT is divided into three partial lengths in Section IV and the total leakage inductance is derived from the combination of the leakage inductances calculated for three different core window arrangements.

The accuracy of the proposed method is confirmed by the 3-D finite element analysis. Moreover, the results of the proposed method are verified by measurements on two constructed MFTs with different core types and dimensions. A sensitivity analysis is also performed, and the results of

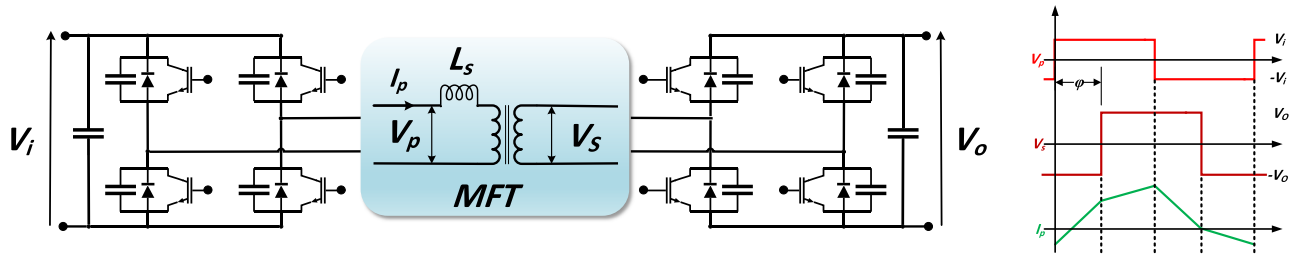

FIGURE 1. Equivalent circuit of a DAB converter and corresponding current and voltage waveforms.

the proposed method are compared with the results of the previous analytical methods as well as the results of the 3-D FEM for various case studies.

II. LEAKAGE INDUCTANCE CALCULATION

A. CALCULATION OF VACTOR POTENTIAL

The geometry used for field analysis is shown in Fig. 2.

The following assumptions are made.

1) The coils are inside the core window and are surrounded by the core walls in the x-y plane.

2) The coils have a rectangular cross section with a uniform current density.

3) The core is assumed to have an infinite permeability which means a flux-normal boundary condition on the core walls.

4) The current density vector **J** is in the z direction and the length of the geometry is infinite in the z-axis direction.

5) The total Ampere-turns of the coils is equal to zero inside the core window.

Since all the field quantities are independent of the z coordinate, the following equation can be used for expressing the vector potential (A) of a coil in planar coordinates.

$$\frac{\partial^2 A}{\partial y^2} + \frac{\partial^2 A}{\partial x^2} = -\mu_0 J \tag{1}$$

The current density inside the coil is constant and can be written as a function of position

$$J(x, y) = \begin{cases} j & x_1 < x < x_2, \quad y_1 < y < y_2 \\ 0 & else \end{cases} \tag{2}$$

where

$$j = \frac{NI}{(x_2 - x_1)(y_2 - y_1)} \tag{3}$$

and NI is the Ampere-turns of the coil.

A double Fourier series can be applied to the current density. To find a correct extension, one needs to consider the boundary conditions at the window walls. Regarding the flux-normal boundary condition at the core walls ($\partial A / \partial n = 0$) and thus the extension required for the vector potential, the following double Fourier series is used for the current density

$$J = \sum_{m=0}^{\infty} \sum_{n=0}^{\infty} J_{mn} \cos(\frac{m\pi}{w_c} x) \cos(\frac{n\pi}{h_c} y) \tag{4}$$

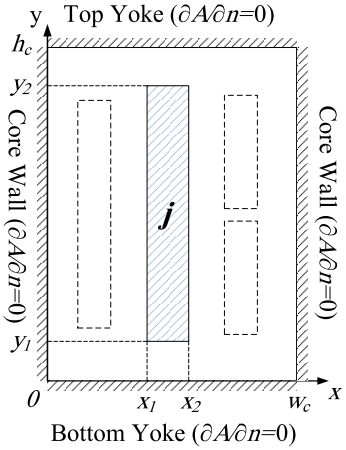

FIGURE 2. The geometry used for field analysis.

The harmonic coefficients (J_{mn}) are calculated as follows.

- Case A: $m = 0, n = 0$

This is the algebraic-average current density inside the core window. Since for the leakage reactance the positive and negative Ampere-turns balance exactly, the sum of J_{00} terms resulting from all coils is equal to zero.

- Case B: $m = 0, n = 1, 2 \ldots$

$$J_{m0} = \frac{2j}{m\pi H} \left(\sin(\frac{m\pi}{w_c} x_2) - \sin(\frac{m\pi}{w_c} x_1) \right) (y_2 - y_1) \tag{5}$$

- Case C: $m = 1, 2 \ldots, n = 0$

$$J_{0n} = \frac{2j}{n\pi L} \left(\sin(\frac{n\pi}{h_c} y_2) - \sin(\frac{n\pi}{h_c} y_1) \right) (x_2 - x_1) \tag{6}$$

- Case D: $m = 1, 2 \ldots, n = 1, 2 \ldots$

$$J_{mn} = \frac{4j}{mn\pi^2} \left(\sin(\frac{m\pi}{w_c} x_2) - \sin(\frac{m\pi}{w_c} x_1) \right) \times \left(\sin(\frac{n\pi}{h_c} y_2) - \sin(\frac{n\pi}{h_c} y_1) \right) \tag{7}$$

Substituting the double Fourier series (4) into (1), we have

$$\frac{\partial^2 A}{\partial y^2} + \frac{\partial^2 A}{\partial x^2} = -\mu_0 \sum_{m=0}^{\infty} \sum_{n=0}^{\infty} J_{mn} \cos(\frac{m\pi}{w_c} x) \cos(\frac{n\pi}{h_c} y) \tag{8}$$

From (8), A can be obtained in the form of a double infinite series as

$$A = \sum_{m=1}^{\infty}\sum_{n=1}^{\infty} A_{mn}\cos(\frac{m\pi}{w_c}x)\cos(\frac{n\pi}{h_c}y) \tag{9}$$

where

$$A_{mn} = \frac{\mu_0 J_{mn}}{(\frac{m\pi}{w_c})^2 + (\frac{n\pi}{h_c})^2} \tag{10}$$

Equation (10) is valid for all values of m and n from 0 to ∞, except for the special case $m = 0$ and $n = 0$. Considering the balanced Ampere-turns inside the core window, there is no need to calculate A_{00} since the product terms of $A_{00}J_{00}$ vanish during leakage inductance calculation.

B. CALCULATION OF LEAKAGE INDUCTANCE PER UNIT LENGTH

Consider N coils (with zero net Ampere-turns) inside the core window as is shown in Fig. 3. The arrangement of the coils is arbitrary. The leakage inductance can be calculated using the total magnetic energy stored inside the core window. The magnetic energy stored in the system is obtained by

$$W = \frac{1}{2}\int AJdv \tag{11}$$

Considering A and J resulting from each coil and substituting A and J with $\sum A_i$ and $\sum J_i$ respectively, the total magnetic energy per unit length is obtained as

$$W^u = \frac{1}{2}\sum_{i=1}^{N}\sum_{j=1}^{N}\int A_i J_j dxdy \tag{12}$$

Considering the core window as the integration area, using (4) and (9), each integral term in (12) can be evaluated as

$$\int A_i J_j dxdy = h_c w_c \left(\frac{1}{4}\sum_{m=1}^{\infty}\sum_{n=1}^{\infty} A_{i_{mn}} J_{j_{mn}} + \frac{1}{2}\sum_{m=1}^{\infty} A_{i_{m0}} J_{j_{m0}} + \frac{1}{2}\sum_{m=1}^{\infty} A_{i_{m0}} J_{j_{m0}}\right) \tag{13}$$

Once the total energy is obtained, the leakage inductance per unit length (H/m) can be obtained as

$$L^u_{leakage} = \frac{2\,W^u}{I^2} \tag{14}$$

where I, denotes the winding current in the side from which the leakage inductance is calculated. It should be noted that in order to obtain the total leakage inductance of the transformer, $L^u_{leakage}$ in (14) should be multiplied by the mean length of turns which is the subject of discussion in the next section.

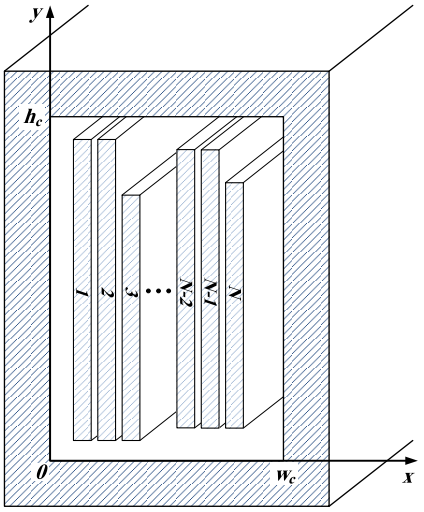

FIGURE 3. Arbitrary arrangement of coils inside the core window.

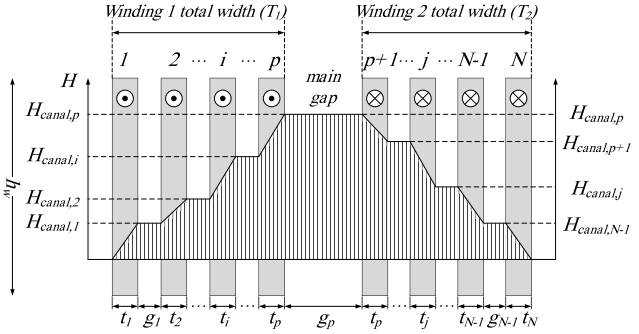

FIGURE 4. Distribution of axial leakage field intensity inside windings.

III. DETERMINATION OF MEAN LENGTH OF TURNS (MLT)

The total leakage inductance is the leakage inductance per unit length multiplied by the mean length of turns (MLT). For this reason, the parameter of MLT is of great importance in the determination of the leakage inductance. Since the method presented here is based on the total energy stored in the axial leakage field of the windings, the calculated MLT is denoted by MLT^{TEM}. The superscript *TEM* stands for the "Total Energy Method".

According to Fig. 4, each winding may have an arbitrary number of coils. It is assumed that all coils of the windings have the same height equal to h_w. The net Ampere-turns is zero and there is no leakage flux outside the windings. The magnetic flux density is calculated using the Ampere law assuming an axial leakage field. The distribution of magnetic field strength, H, inside the windings and in the main gap is demonstrated in Fig. 4. The magnetic field strength is constant inside the gaps while it changes linearly inside the coils

$$H_{canal_k} = \frac{1}{h_w}\sum_{i=1}^{k} NI_i \tag{15}$$

$$H_{coil_k} = H_{canal_{k-1}} + \frac{NI_k}{h_w}\frac{x}{t_k} \tag{16}$$

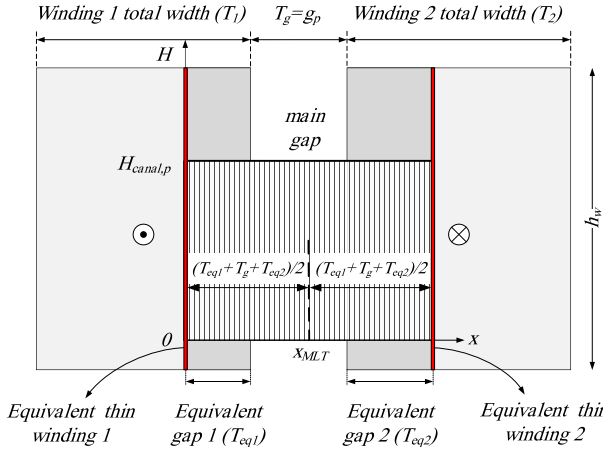

FIGURE 5. The windings are replaced with equivalent gaps and equivalent thin windings to make a gap with a uniform field intensity equal to the filed intensity of the main gap and with an energy equal to the total energy of the leakage field.

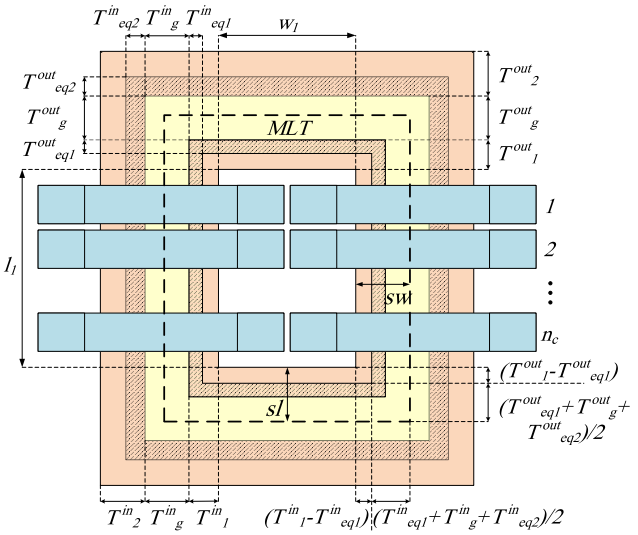

FIGURE 6. Determination of the MLT (named MLT^{TEM}) considering the winding parameters.

where NI_k is the Ampere-turns of the coil k and t_k is the width of the coil k.

The stored energy (per unit length) in each winding is the sum of the energies stored inside the coils and the gaps between the coils

$$W_1^u = \sum_{k=1}^{p} \int_0^{t_k} \frac{1}{2}\mu_0 H_{coil_k}^2 h_w dx + \sum_{k=1}^{p-1} \frac{1}{2}\mu_0 H_{canal_k}^2 h_w g_k \quad (17)$$

$$W_2^u = \sum_{k=p+1}^{N} \int_0^{t_k} \frac{1}{2}\mu_0 H_{coil_k}^2 h_w dx + \sum_{k=p+1}^{N-1} \frac{1}{2}\mu_0 H_{canal_k}^2 h_w g_k \quad (18)$$

where g_k is the gap size between the coils k and $k+1$. Note that g_p is the size of the main gap. The field strength is constant in the main gap and thus the stored energy in the main gap is given by

$$W_G^u = \frac{1}{2}\mu_0 H_{canal_p}^2 h_w g_p \quad (19)$$

where

$$H_{canal_p} = \frac{NI_{W1}}{h_w} = -\frac{NI_{W2}}{h_w} \quad (20)$$

and NI_{W1} is the total Ampere-turns of winding 1 and NI_{W2} is the total Ampere-turns of winding 2.

If windings 1 and 2 are replaced by equivalent windings with infinitely small width but with the same Ampere-turns (see Fig. 5), the field intensity in the gap between two equivalent windings will have a constant value. In this case, to have a field intensity equal to $H_{canal,p}$ (the value of the field intensity in the main gap), the width of the gaps added to the sides of the main gap (namely the equivalent gaps 1 and 2) should be determined in such a way that the stored energy in the equivalent gaps 1 and 2 to be the same as the energy stored inside windings 1 and 2 respectively. According to Fig. 5, the energies stored in the equivalent gaps are given by

$$W_1^u = \frac{1}{2}\mu_0 H_{canal_p}^2 h_w T_{eq_1} \quad (21)$$

$$W_2^u = \frac{1}{2}\mu_0 H_{canal_p}^2 h_w T_{eq_2} \quad (22)$$

where T_{eq1} and T_{eq2} are the widths of the equivalent gap of windings 1 and 2 respectively.

Equating (17) with (21) and (18) with (22), after some algebraic simplifications, T_{eq1} and T_{eq2} are obtained as

$$T_{eq_1} = \frac{1}{H_{canal_p}^2}\sum_{k=1}^{p}\left(H_{canal_{k-1}}^2 t_k + \frac{t_k}{3}\frac{NI_k^2}{h_w^2} + \frac{H_{canal_{k-1}}}{h_w} NI_k t_k\right) + \frac{1}{H_{canal_p}^2}\sum_{k=1}^{p-1}\left(H_{canal_k}^2 g_k\right) \quad (23)$$

$$T_{eq_2} = \frac{1}{H_{canal_p}^2}\sum_{k=p+1}^{N}\left(H_{canal_{k-1}}^2 t_k + \frac{t_k}{3}\frac{NI_k^2}{h_w^2} + \frac{H_{canal_{k-1}}}{h_w} NI_k t_k\right) + \frac{1}{H_{canal_p}^2}\sum_{k=p+1}^{N-1}\left(H_{canal_k}^2 g_k\right) \quad (24)$$

According to Fig. 6, knowing T_{eq} for windings 1 and 2 inside and outside the core window, the MLT can be determined using the parameters sw and sl which are calculated as follows.

$$sw = T_1^{in} - T_{eq_1}^{in} + \left(T_{eq_1}^{in} + T_g^{in} + T_{eq_2}^{in}\right)/2 \quad (25)$$

$$sl = T_1^{out} - T_{eq_1}^{out} + \left(T_{eq_1}^{out} + T_g^{out} + T_{eq_2}^{out}\right)/2 \quad (26)$$

where T_{eq1}^{in} and T_{eq1}^{out} are the widths of the equivalent gap of winding 1 inside and outside the core window respectively, and likewise T_{eq2}^{in} and T_{eq2}^{out} are the widths of the equivalent gap of winding 2 inside and outside of the core window respectively. Note that the width of each winding inside or outside the core window (indicated by T_1^{in}, T_1^{out}, T_2^{in} and T_2^{out}) is equal to the sum of the widths of the corresponding coils and gaps inside or outside the core window.

In general, in the presented method for calculation of the MLT, all the gaps including the main gap can have arbitrary values inside and outside the core window. In a case where each winding consists of one coil and the widths of the windings are also identical, the MLT path will go through the middle of the main gap for all sides. If this is not the case, depending on the parameters *sw* and *sl*, the MLT path will deviate from the middle of the main gap which will result in a change of the mean length of turns and consequently a different value of the total leakage inductance of the transformer.

Using the obtained relations for the stored energy inside the windings and in the main gap, it is possible to derive a relation for the leakage inductance of the planar MFTs similar to the classical relations presented in literature for conventional power transformers [16]. For this purpose, it is assumed that the leakage flux is in the axial direction while the Rogowski factor is applied subsequently for taking the radial component of the leakage flux into account. If $L_{leakage,1D}^{u,in}$ is the leakage inductance per unit length inside the core window and $L_{leakage,1D}^{u,out}$ is the leakage inductance per unit length outside the core window (both in H/m), the total leakage inductance is given by

$$L_{leakage} = k_r^{in} l^{in} L_{leakage,1D}^{u,in} + k_r^{out} l^{out} L_{leakage,1D}^{u,out} \quad (27)$$

where k_r^{in} and k_r^{out} are the Rogowski factors inside and outside the core window and l^{in} and l^{out} are the mean length of turns inside and outside the core window (in m) respectively. The l^{in} and l^{out} parameters are calculated as

$$l^{in} = 2(l_1 + 2\,sl) \quad (28)$$

$$l^{out} = 2(w_1 + 2\,sw) \quad (29)$$

where l_1 and w_1 are indicated in Fig. 6. Using the amount of energy stored inside the windings and in the main gap, $L_{leakage,1D}^{u,in}$ and $L_{leakage,1D}^{u,out}$ are calculated as

$$L_{leakage,1D}^{u,in} = 2\left(W_1^{u,in} + W_G^{u,in} + W_2^{u,in}\right)\Big/ I^2 \quad (30)$$

$$L_{leakage,1D}^{u,out} = 2\left(W_1^{u,out} + W_G^{u,out} + W_2^{u,out}\right)\Big/ I^2 \quad (31)$$

where $W_1^{u,in}$ and $W_1^{u,out}$ are obtained from (21) by replacing T_{eq} with T_{eq1}^{in} and T_{eq1}^{out}. Similarly, $W_2^{u,in}$ and $W_2^{u,out}$ are obtained from (22) by replacing T_{eq} with T_{eq2}^{in} and T_{eq2}^{out} and also $W_G^{u,in}$ and $W_G^{u,out}$ are obtained from (19) by replacing g_p with T_g^{in} and T_g^{out}, respectively. I is the current of the excited winding.

The Rogowski factor inside the core window, k_r^{in}, is obtained as [17]

$$k_r^{in} = 1 - \frac{1 - e^{-\frac{\pi h_w}{(T_1^{in}+T_g^{in}+T_2^{in})}}}{\pi h_w \big/ (T_1^{in} + T_g^{in} + T_2^{in})} \quad (32)$$

To calculate k_r^{out}, the Rogowski factor outside the core window, the superscript "*in*" is replaced with "*out*" in (32). Note that (27) is the relation for the leakage inductance calculation based on the classical approach and the "in" and "out" superscripts in (27) are only for the possibility of having different main gaps inside and outside the core window. The mentioned superscripts are not for considering the different boundary conditions (introduced by the core walls) inside and outside the core window.

According to the method described for the classical method, l^{in} and l^{out} are independent of h_w but the total leakage inductance is dependent on h_w according to (19), (21) and (22). If the heights of windings 1 and 2, h_{w1} and h_{w2}, are different, then h_w can be calculated as the average height of the windings i.e., $(h_{w1} + h_{w2})/2$. If each winding itself consists of a number of coils with different heights, then the maximum height covered by the coils, not the average height of the coils, is considered as the height of that winding. The simulation results show that the calculation of h_{w1} and h_{w2} in this way leads to much better results than the case where h_{w1} and h_{w2} are considered as the average heights of the coils. It should be noted that the method described for determining h_w is dedicated only to the classical method developed in this section whereas in the method presented in Section II which is based on a two-dimensional field analysis, the height of each coil is accurately considered in the calculations.

IV. SEGMENTATION OF MLT AND LEAKAGE INDUCTANCE CALCULATION

According to Fig. 7, the MLT path, defined in Section III, can be divided into three different parts, namely MLT_{in}, MLT_{out1} and MLT_{out2}. Over the length of MLT_{in}, the windings are surrounded completely by the core walls. Over the length of MLT_{out1}, the windings are adjacent to the core walls only from one side and over the length of MLT_{out2} where the windings are not adjacent to the core walls from left or right side, there is no major effect from the core walls on the leakage inductance. Based on this partitioning, the leakage inductance is calculated with three different arrangements of the core window as it is shown in Fig. 8. The arrangement shown in Fig. 8(a) is used to calculate the leakage inductance for those parts of the windings which are situated completely inside the core window and have a total length equal to MLT_{in}.

To calculate the leakage inductance for MLT_{out1}, as shown in Fig. 8(b), the outer wall of the core window is displaced in the radial direction while the upper and lower walls of the core window are displaced axially in opposite directions. The amount of displacement in the radial direction is the same as the width of the core window that is enough to neutralize the effect of the core's outer wall. The displacements of the upper

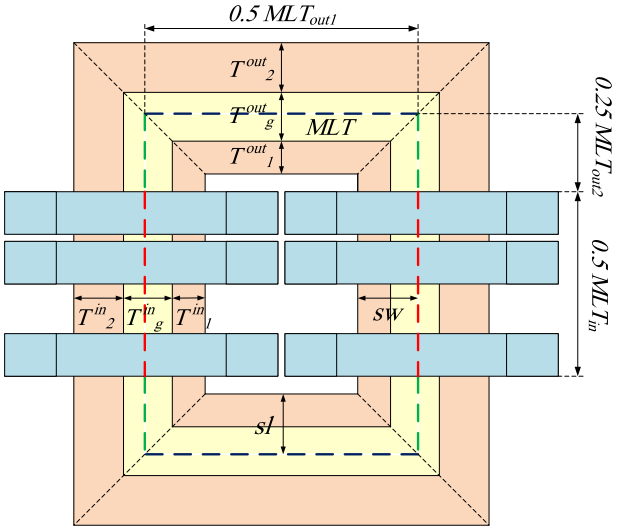

FIGURE 7. Segmentation of the MLT into three partial lengths, MLT_{in}, MLT_{out1} and MLT_{out2} ($MLT=MLT_{in}+MLT_{out1}+MLT_{out2}$).

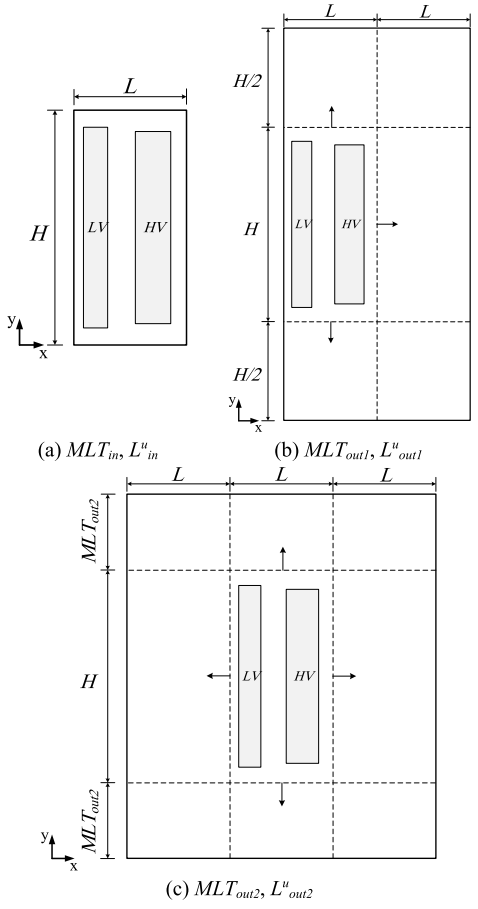

FIGURE 8. Core window arrangements and the relevant partial lengths and the corresponding leakage inductances (a) actual core window (b) core window with displaced core walls used for the region out1 (c) core window with displaced core walls used for the region out2.

and lower walls are also in such a way that the window height in the new case is twice the actual height of the core window. This ensures that the yoke impact on leakage inductance is small enough for MLT_{out1}.

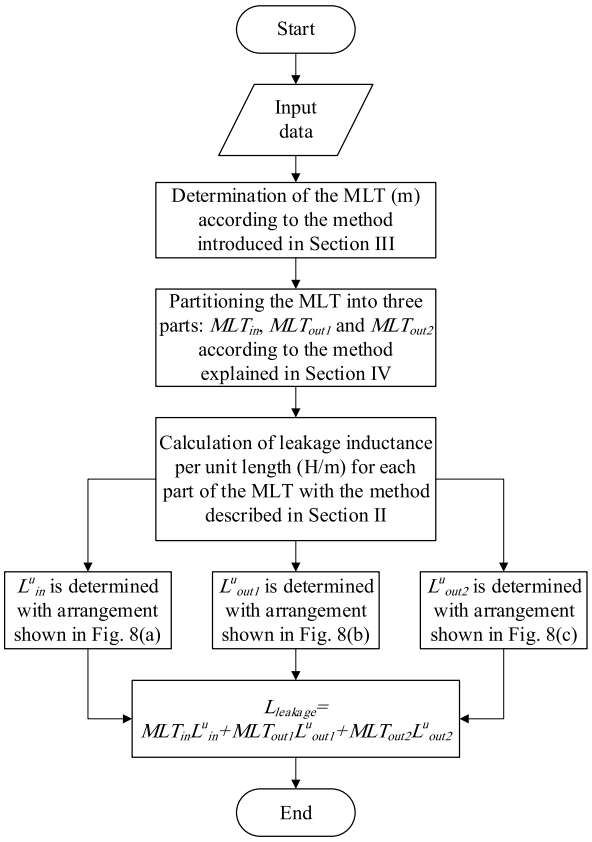

FIGURE 9. The proposed method used for calculation of the leakage inductance.

For MLT_{out2} the effect of the iron core is smaller and thus, the inner and outer walls of the core window are assumed to be far enough away from the windings. The suitable displacement of the core walls for this part is demonstrated in Fig. 8(c). The displacements of the upper and lower walls of the core window are equal to MLT_{out2} implying that the effect of yokes becomes smaller as MLT_{out2} increases so that the effect of yokes vanishes as MLT_{out2} tends to infinity. If the leakage inductances corresponding to the core window arrangements in Figs. 8(a), 8(b) and 8(c) are L^u_{in}, L^u_{out1} and L^u_{out2} respectively, the total leakage inductance is obtained as

$$L_{leakage} = MLT_{in}L^u_{in} + MLT_{out1}L^u_{out1} + MLT_{out2}L^u_{out2} \quad (33)$$

The proposed method for the leakage inductance calculation is illustrated by a flowchart in Fig. 9. The procedure includes determination of the MLT according to the method presented in Section III, dividing the obtained MLT into three parts according to the method presented in this section and calculation of the leakage inductance per unit length for each part based on the analytical approach presented in Section II and then obtaining the total leakage inductance by (33).

V. FEM SIMULATION

In order to validate the proposed method, the 3-D finite element method is employed to analyze the leakage field inside the MFTs under study. Two MFTs are studied in this paper,

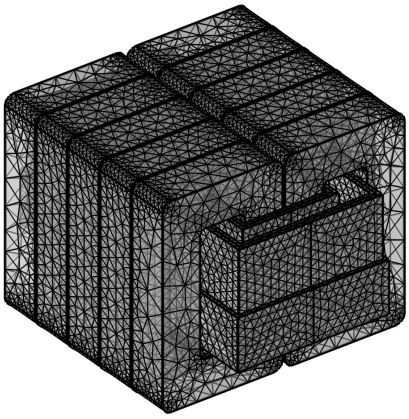

FIGURE 10. The mesh results for the Ferrite-core MFT.

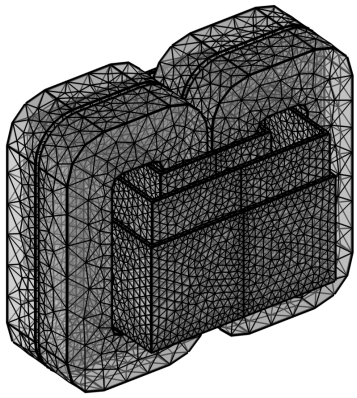

FIGURE 11. The mesh results for the Nanocrystalline-core MFT.

one with a Ferrite core and another with a Nanocrystalline core. COMSOL Multiphysics is used for the field analysis. Since the winding layers do not have the same dimensions, they are considered as individual coils with a gap equal to the thickness of the inter-layer insulation tape between them. Each winding layer is defined as a stranded coil with a certain number of turns. The currents of the windings are specified in such a way that the net Ampere-turns is equal to zero to comply with the short-circuit test condition used for measuring the leakage inductance. As a result, the amplitude of the main flux in the core is low and the working point is on the linear part of the core's magnetization curve i.e., the core acts as a linear magnetic material. For this reason, the core has been modeled with a sufficiently large relative permeability (e.g., μ_r=1000) without taking saturation phenomena into account. The windings and the surrounding medium are modeled with μ_r=1. Furthermore, due to the usage of Litz wire in the windings, it can be assumed that the current density is uniformly distributed inside the windings. The electrical conductivity of all materials is set to be zero. The mesh results for the Ferrite-core and Nanocrystalline-core MFTs are presented in Figs. 10 and 11, respectively. The surrounding medium is made hidden to make the active part more visible.

The leakage flux distributions obtained from the magnetic analysis for the Ferrite-core and Nanocrystalline-core MFTs are shown in Figs. 12 and 13 respectively. As is clear from these figures, the presence of a high-permeable core changes the shape of the leakage flux affecting the leakage inductance consequently. The leakage flux has a significant outward fringing in the region where the windings are not surrounded by the core walls.

The distributions of magnetic flux density in different cut planes (defined in Fig. 14) are illustrated in Fig. 15. As is clear from Fig. 15(a), in cut plane 1, the windings are surrounded by the core walls from all sides, contributing to a high leakage inductance especially due to the axial leakage flux resulting from the high-permeable top and bottom yokes. As can be seen from Fig. 15(b), in cut plane 2, the windings

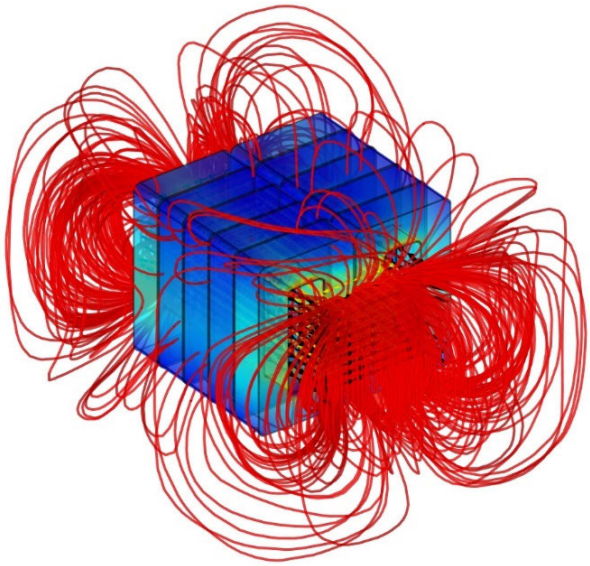

FIGURE 12. The result of 3-D FEM simulation for leakage field analysis of the Ferrite-core MFT.

are adjacent to the core wall only from one side, resulting in a lower leakage inductance due to an increase in the radial component of the leakage flux. In cut plane 3, as is shown in Fig. 15(c), the windings are not adjacent to any of the core walls, accordingly resulting in a much lower leakage inductance. It can be seen that the leakage flux pattern in cut plane 3 is clearly different from the one in cut plane 2 where the side core wall deforms the leakage flux considerably.

The results of the leakage inductance calculation using the proposed method and using FEM (referred to the low-voltage side) are given in Table 1. The larger error with the Nanocrystalline-core MFT in Table 1 can be related to its larger main gap which results in an increase in the radial component of the leakage field. In the finite element method, the leakage inductance is calculated using the total stored magnetic energy. Note that due to the low level of flux in the core, the energy stored inside the core is very low and therefore the total magnetic energy is in principle equal to the energy stored in the leakage field. The per-unit-length leakage

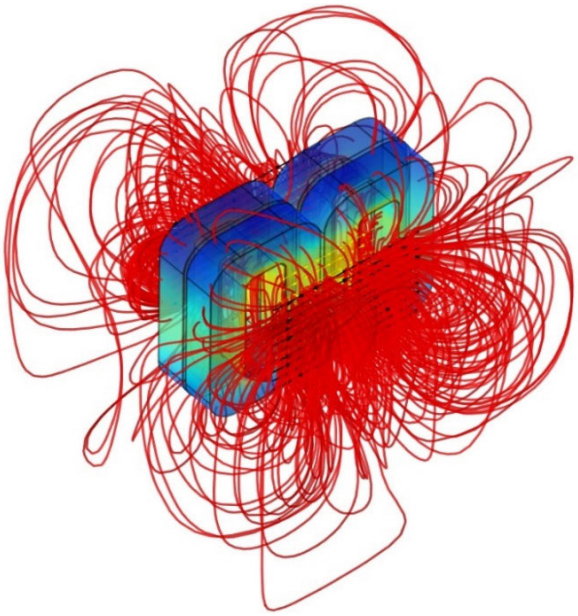

FIGURE 13. The result of 3-D FEM simulation for leakage field analysis of the Nanocrystalline-core MFT.

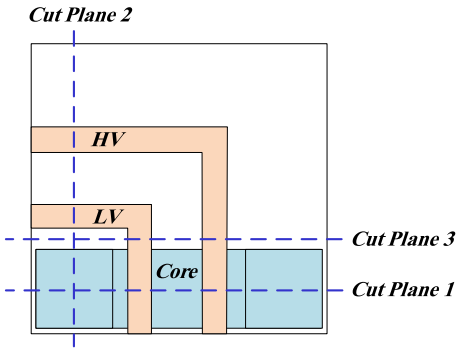

FIGURE 14. Cut planes in the corner of the model (from top view) for demonstrating the distribution of the leakage field in different regions.

TABLE 1. Results of leakage inductance calculation.

	Ferrite	Nanocrystalline
3-D FEM (μH)	40.63	30.85
proposed method (μH)	40.64	30.77
proposed method error relative to 3-D FEM (%)	0.0	0.3

inductances and the corresponding MLT partial lengths calculated by the proposed method are also provided in Table 2. As can be seen from Table 1, the error of the proposed method related to FEM is less than 1% for both MFTs. This level of accuracy proves efficiency of the proposed method provided in this article for calculating the leakage inductance of shell-type MFTs with rectangular windings.

VI. TEST OBJECT AND EXPERIMENTAL VERIFICATION

To verify the proposed method, inductance measurements have been performed on two fabricated 50 kW, 1 kV to 3 kV shell type MFTs, one with a Ferrite core and another with a Nanocrystalline core [33]. The prototypes are shown in Fig. 16. Note that the high frequency content of the

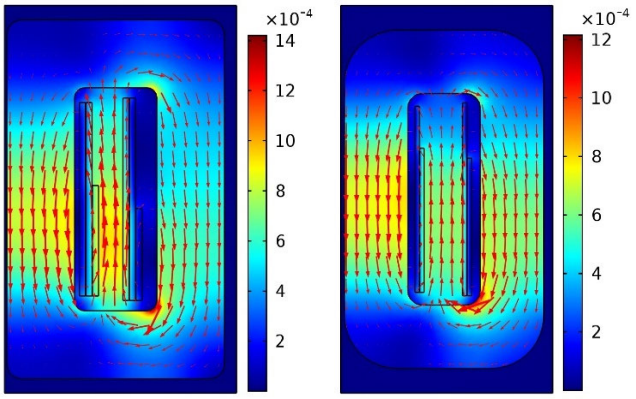

(a) Leakage field in cut plane 1, associated with MLT_{in}

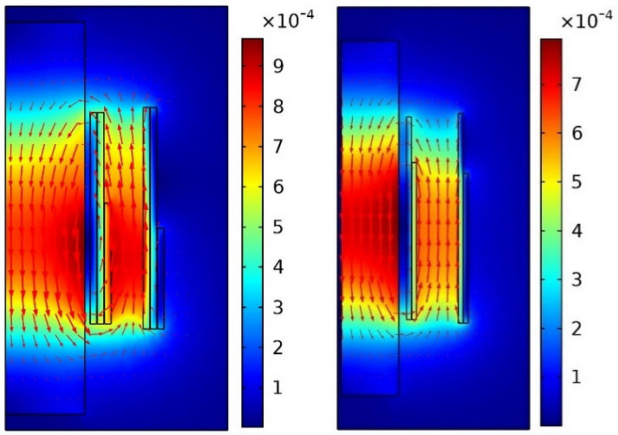

(b) Leakage field in cut plane 2, associated with MLT_{out1}

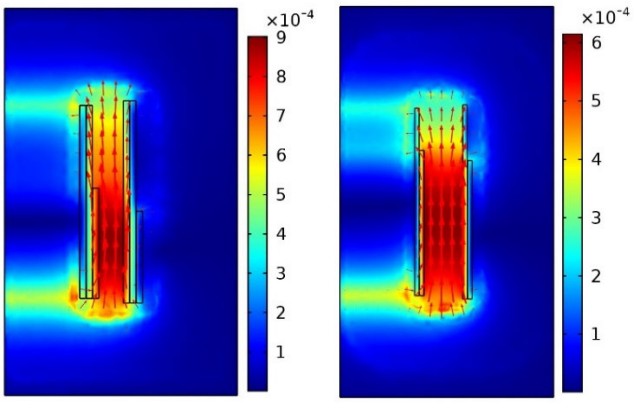

(c) Leakage field in cut plane 3, associated with MLT_{out2}

FIGURE 15. Distribution of leakage field (T) in the cut planes for two MFT prototypes (right plots for Ferrite-core MFT and left ones for Nanocrystalline-core MFT).

voltage waveform applied to the MFT windings necessitates the use of a magnetic core with low AC losses at high frequencies. Therefore, a set of 5 pairs of Ferrite magnetic cores and a set of 2 pairs of Nanocrystalline magnetic cores are used for the prototypes. To minimize the high frequency eddy current losses in the windings, a Litz-type wire consisting of 181 copper strands, each with diameter of 0.2 mm, is used. The dimensions of Litz wire used are 3.8 mm × 2.5 mm.

TABLE 2. Per-unit-length leakage inductances (μH/m) and the MLT partial lengths (mm) calculated by the proposed method.

Ferrite			Nanocrystalline		
L^u_{in}	L^u_{out1}	L^u_{out2}	L^u_{in}	L^u_{out1}	L^u_{out2}
73.591	76.636	65.804	74.387	68.942	66.272
MLT_{in}	MLT_{out1}	MLT_{out2}	MLT_{in}	MLT_{out1}	MLT_{out2}
316.00	173.79	61.786	128.00	231.62	79.62

FIGURE 16. The MFT prototypes used as the test objects (Ferrite-core MFT on the left side and Nanocrystalline-core MFT on the right side).

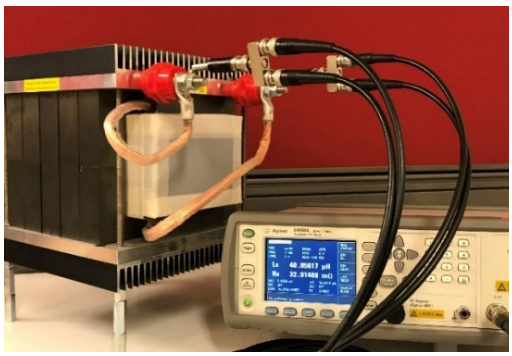

FIGURE 17. The test setup for leakage inductance measurement.

In the Ferrite-core MFT, the LV winding has 18 turns with 3 parallel wires in axial direction for each turn and it is wound in three layers. The HV winding has 54 turns, and it is built in three layers with 1 wire for each turn. In the Nanocrystalline-core MFT, the LV winding has 16 turns with 3 parallel wires in axial direction for each turn and it is wound in two layers. The HV winding has 48 turns, and it is built in two layers with 1 wire for each turn. The rated currents of the LV and HV windings in both MFTs are 54 and 18 A respectively. The detailed parameters of the fabricated MFT prototypes are presented in the APPENDIX.

The measurement of leakage inductance is performed using an Agilent E4980A RLC meter. To minimize the measurement error, the E4980A RLC meter features powerful correction functions including cable length correction as well as load corrections. These correction functions are used to correct additional errors introduced by the test fixture and the test leads. Also, by an effective shielding, the effects of the electrical noise picked up by the test leads are minimized.

The test setup is shown in Fig. 17. The measurements are performed from the LV winding while the HV winding is

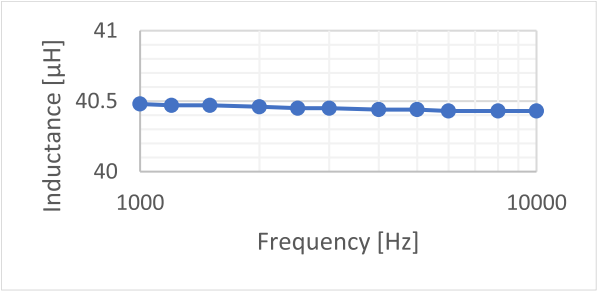

FIGURE 18. The leakage inductance measured as a function of frequency for the Ferrite-core MFT.

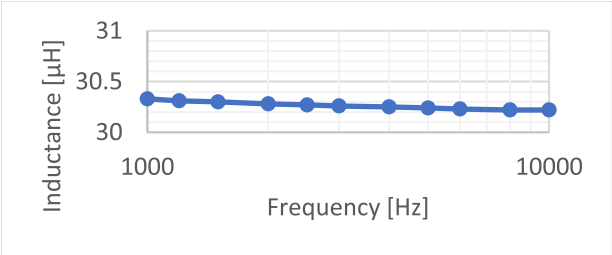

FIGURE 19. The leakage inductance measured as a function of frequency for the Nanocrystalline-core MFT.

short-circuited. The leakage inductance values measured in the frequency range of 1 kHz to 10 kHz are demonstrated in Figs. 18 and 19. As can be seen from these figures, the leakage inductance does not change significantly in the measurement frequency range. This confirms that the leakage inductance is not affected by the skin and proximity effects due to the use of Litz wire in the windings.

It is noted that the skin depth ($\delta = \sqrt{2/(\omega\mu\sigma)}$ [34]) of copper at 10 kHz is about 0.73 mm (with $\sigma = 4.74e7$ S/m at 75°C) while the diameter of each strand of Litz wire is only 0.2 mm. Therefore, due to the small diameter of the conductor strands compared to the depth of penetration, no significant change is observed in the leakage inductance in the frequency range of 1 kHz to 10 kHz.

The results of the leakage inductance measurement are presented in Table 3. The average measured value for the leakage inductance according to measurements is 40.44 μH for the MFT with Ferrite core and 30.24 μH for the MFT with Nanocrystalline core. It can be noticed from Table 3 that the leakage inductances computed using the 3-D FEM and using the proposed method are in close agreement to the measurement results.

It can also be seen from Table 3 that despite considering the most details of geometry, there is still a small difference between the results of the 3-D FEM and the measurement in the case of the MFT with Nanocrystalline core. Since substantial efforts have been made to minimize the measurement error, the remaining error is believed to be due to the tolerances of the manufacturing process. However, if the 3-D FEM is used as the reference method, it can be seen that the proposed method is very accurate according to Table 1.

TABLE 3. Results of leakage inductance calculation.

	Ferrite	Nanocrystalline
Measurement (μH)	40.44	30.24
3-D FEM (μH)	40.63	30.85
Proposed Method (μH)	40.64	30.77
3-D FEM Error Relative to Measurement (%)	0.5	2.0
Proposed Method Error Relative to Measurement (%)	0.5	1.8

VII. SENSITIVITY ANALYSIS

To verify the proposed method, a sensitivity analysis is performed on both MFTs with Nanocrystalline and Ferrite cores. According to Fig. 20, four cases are considered for each MFT. The first case is equivalent to the actual dimensions of the transformer. As the second case, the gaps between the LV winding's layers are increased so that $g = 5$mm while all the other distances including the main gap and the HV winding's clearances are kept constant. The increased gaps are for creating oil ducts and improving the cooling of the LV winding at higher currents. As the third case, the HV winding clearances are increased so that the distances d_1 and d_2 are equal to 22 and 36 mm, respectively. This is accomplished by moving the HV winding to the right side and displacing the core walls accordingly. Increasing HV winding clearances is for enhancing the insulation withstand of the HV winding at higher voltages. The fourth case is the combination of the second and third cases. In this case, the gaps between the LV layers and the HV winding's clearances are increased simultaneously. This case represents the geometrical conditions required for the operation of a high-power high-voltage MFT. The leakage inductance is calculated using different methods for both MFTs for the aforementioned four cases. The relative errors are presented in Table 4. The 3D FEM is used as the reference method and the other methods are compared with it. Note that due to the dimensional limitation of the existing off-the-shelf cores, it was not practical to build and test all the cases studied in the sensitivity analysis.

The results of the 3-D FEM are highlighted by gray color. The error values of more than 1% are highlighted by orange color. It can be seen that the error of the method of inductance calculation with MLT^{TEM} divided in three parts i.e., MLT_{in}, MLT_{out1} and MLT_{out2}, is less than 1 % for both MFTs in all cases. This indicates the high accuracy of the proposed method for the leakage inductance calculation. Note that the proposed method is according to the procedure illustrated by the flowchart in Fig. 9.

To investigate the effect of the segmentation of the MLT which is discussed in Section IV, another simulation is performed, and its results are presented in Table 4. In this simulation, MLT^{TEM} is divided into two segments, MLT_{in} and MLT_{out}, instead of three segments. Here, MLT_{out} is the sum of MLT_{out1} and MLT_{out2} (see Fig. 7) and the arrangement shown in Fig. 8(b), which is the arrangement used for MLT_{out1} in the previous simulation, is used to calculate the leakage inductance for MLT_{out}. The errors introduced in this case

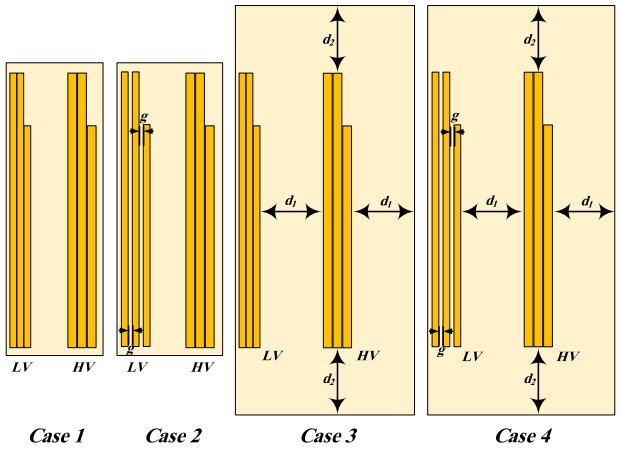

FIGURE 20. The different arrangements of the windings used in sensitivity analysis.

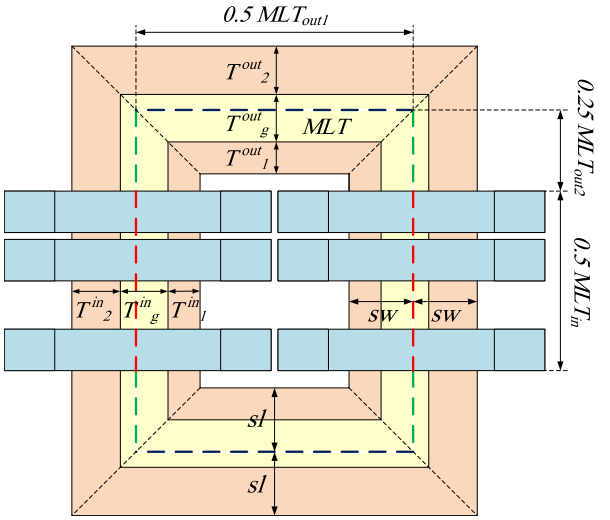

FIGURE 21. The MLT in the middle of the sum of the widths of the windings and the main gap (named MLT^{MTW}). sl=$(T_1^{out} + T_g^{out} + T_1^{out})/2$, sw=$(T_1^{in} + T_g^{in} + T_1^{in})/2$.

confirm the importance of a correct segmentation of the MLT for the leakage inductance calculation.

The effect of the MLT's determination method on the leakage inductance has been also investigated in the sensitivity analysis. For this purpose, according to Fig. 21, the middle of the total width of the windings and the main gap is used to determine the MLT (MLT^{MTW}). This is the way usually used for determining the MLT [31]. Similar to MLT^{TEM}, the leakage inductance calculation with MLT^{MTW} has been performed with a 2-part MLT as well as a 3-part MLT and the results are presented in Table 4. The calculation results show that considerable errors are introduced for both MFTs as a result of using MLT^{MTW} instead of using MLT^{TEM} (the MLT proposed in the paper). Since the mean length of turns is not assessed correctly with MLT^{MTW}, segmentation of the MLT in 2 or 3 parts does not make any difference in the accuracy i.e., both 2-part and 3-part MLTs are not accurate enough in this case.

TABLE 4. Leakage inductance results from the sensitivity analysis.

				Ferrite				*Nano*			
				Case 1	*Case 2*	*Case 3*	*Case 4*	*Case 1*	*Case 2*	*Case 3*	*Case 4*
3-D FEM (μH)				40.63	52.60	66.18	77.04	30.85	34.19	30.17	33.22
Error of 2D-planar method (%)	*with* MLT^{TEM}	divided in 3 parts	√	0.0	0.4	0.5	0.9	-0.3	- 0.2	0.1	0.3
		divided in 2 parts *	×	1.7	2.3	1.9	2.5	0.4	0.6	1.5	1.9
	with MLT^{MTW}	divided in 3 parts	×	0.7	-2.5	1.1	-1.9	0.1	-2.5	0.4	-2.1
		divided in 2 parts *	×	2.4	-0.9	2.6	-0.5	0.8	-1.8	1.9	-0.6
Error of adopted classical method (%)	*with* MLT^{TEM}		×	-2.9	-1.7	4.3	7.3	-2.9	-1.8	0.2	1.9
	with MLT^{MTW}		×	-2.2	-4.9	5.0	4.0	-2.5	-4.2	0.6	-0.6

The error's background color: white for equal to or smaller than 1% and orange for larger than 1%.
* $MLT_{out}=MLT_{out1}+MLT_{out2}$; the arrangement shown in Fig. 8(b) is used for MLT_{out}

It should be noted that since the actual widths of the LV and HV windings are the same in both MFTs, MLT^{MTW} in cases 1 and 3 (cases without increasing gaps between LV layers) is approximately equal to MLT^{TEM} and thus, the errors with the 3-part MLT^{MTW} in cases 1 and 3 are noticeably small. Finally, the results of the leakage inductance calculation using the classical method detailed in Section III are added to Table 4. The results demonstrate that, depending on the arrangement of the core and the coils, this method can result in considerable errors in the leakage inductance calculation for both MLT^{TEM} and MLT^{MTW}. Although employment of the classical method is simpler, it is not suitable for calculation of the leakage inductance of the shell type MFTs.

The results of the sensitivity analysis show that the leakage inductance is calculated accurately in all cases using the proposed method. In summary, it can be concluded that calculation of the leakage inductance per unit length, determination of the MLT and the MLT's segmentation, all should be done correctly for an accurate estimation of the leakage inductance.

Regarding the computation time required for the calculations, it can be seen from (13) that the relation obtained for the leakage inductance per unit length is in the form of a double infinite series and therefore the total computation time is strongly dependent on the number of components used in estimating the value of the series. To achieve an accuracy up to two decimal places and therefore the lowest cut-off error, 50 components for each of x and y variables is used to determine the leakage inductance. By reducing this number, the calculation cost can be significantly improved with a relatively small reduction in the accuracy. Therefore, depending on the acceptable criterion for the error value, the computation time is variable. The computation time of the proposed method is also a function of the number of winding layers (coils) used in the leakage inductance calculation. By increasing the number of winding layers, the computation time is increased too. Since the layers inside each winding do not have the same dimensions, the leakage inductance is calculated considering the individual layers of the windings for both MFTs.

According to Table 5, the total computation time for the proposed method is assessed about 0.36 and 0.75 s for MFTs with Nanocrystalline and Ferrite cores, respectively. Note that these times correspond to the total times required for calculating the leakage inductance for a 3-part MLT (with three core window arrangements) and thus the approximate solution times for one core window arrangement are about 0.12 and 0.25 s. Note that the computation times are different because the numbers of winding layers are different in two MFTs. It is noteworthy that the solution time is reduced to about 0.072 millisecond if each of the LV and HV windings is represented with one single coil instead of a layer-by-layer modeling, however, at the cost of decreasing the accuracy. The computation time as a result of using the 2-D magnetostatic FEM for calculation of the leakage inductance per unit length is also presented in Table 5. Note that the 2-D FEM is only used for calculating the leakage inductance per unit length while the total leakage inductance is calculated using the 3-part MLT^{TEM} according to the method proposed in this paper. It can be seen that the computation time of the 2-D FEM is in the order of several seconds while the analytical method takes less than of 1 second in the case of both MFTs. The equivalent 3-D FEM simulations in the same PC used for the proposed method take nearly 10 and 8 minutes to run for two MFTs under study. Note that in order to reduce the solution time and facilitate performing multiple 3-D FEM simulations, the geometry of the core for the 3-D FEM simulations is simplified by neglecting the small distances between the core stacks to model the core as a bulk magnetic material. It should be noted that in addition to the solution time, the use of the finite element method (2-D or 3-D) requires some pre- and postprocessing steps such as drawing the geometry, meshing the model and extracting the results, which make the repeatability of the analysis more challenging. Moreover, using the finite element method requires a software or tool that is not always available for everyone.

TABLE 5. Comparison of the calculation time for different methods.

Nanocrystalline-core MFT (with 4 winding layers)			Ferrite-core MFT (with 6 winding layers)		
Proposed analytical method	Proposed method with 2-D FEM	3-D FEM	Proposed analytical method	Proposed method with 2-D FEM	3-D FEM
0.36 s	9 s	8 min	0.75 s	9.6 s	10 min

To sum up, the 3-D FEM is very accurate, but it requires a considerable solution time when a large number of simulations needs to be run to evaluate the design variants of

a transformer. The analytical method is much faster, and it is easy to implement, making it possible a more advanced optimization with a shorter time. The 2-D magnetostatic FEM can also be used for calculation of leakage inductance per unit length, however, at the cost of much longer solution time compared to the analytical approach. The classical method is fastest (in the order of several milliseconds, not shown in Table 5) compared to the other methods but it is not accurate enough to employ to a MFT.

VIII. CONCLUSION

In this paper, an accurate analytical method for the leakage inductance calculation of shell-type E-core transformers with rectangular windings is presented. The expression derived for the leakage inductance per unit length is based on a double Fourier series expansion of the field inside the core window. The method is applicable to any arbitrary arrangement of windings inside the core window, taking the radial as well as the axial component of the leakage field into account. It was shown that the classical method, due to neglecting the core's effect and also simplifications made in the problem's geometry, is not suitable to apply to the shell-type MFTs used in DAB converters.

In 2-D methods, the total leakage inductance is obtained by multiplying the leakage inductance per unit length by the mean length of turns (MLT). The simulation results reveal that the conventional method for determining the MLT is not accurate enough in the case of MFTs in general. In this paper, a new method based on the total energy stored in the axial leakage field is presented by which the MLT can be determined more accurately considering the distribution of Ampere-turns inside individual layers of the windings. It was also shown that by dividing the MLT into three partial lengths and combining the corresponding leakage inductances according to the method presented in the paper, the accuracy of the leakage inductance calculation can be enhanced significantly.

The proposed method has been verified by 3-D FEM simulations. The error is less than 1% compared to the 3-D FEM in all studied cases. The accuracy of the proposed method, unlike for the previous methods, is not affected by the dimensions of the core and windings. The results of the sensitivity analysis show that despite the accurate determination of the leakage inductance per unit length, the lack of accurate determination of the MLT can lead to an error of 2.6%. It is also concluded that by considering the boundary conditions exerted by the core walls to different parts of the windings, the error of leakage inductance calculation can improve by about 2.5%. The proposed method is also employed to two MFT prototypes and the results are experimentally verified. The comparisons confirm the accuracy of the proposed method for actual high-power MFTs. The 3-D FEM simulation is very accurate, but it is also very time consuming. The analytical method proposed in this paper is, however, easy to implement and can be used to examine a large number of designs in a short time with high accuracy.

APPENDIX

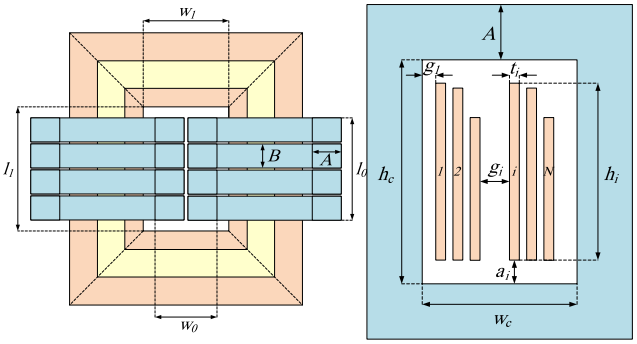

FIGURE 22. The parameters of the shell-type transformer prototypes.

TABLE 6. The properties of the shell-type transformer prototypes.

	Layer No.	t	g_{in}	g_{out}	h	a	N	I
Ferrite w_c=34, h_c=92, A=28, B=30, w_0=58, l_0=158, w_1=62, l_1=162	1	2.5	2	2	79.8	6.1	7	54
	2	2.5	0.2	0.2	79.8	6.1	7	54
	3	2.5	0.2	0.2	45.6	6.1	4	54
	4	2.5	10.1	12.1	83.6	4.2	22	-18
	5	2.5	0.2	0.2	83.6	4.2	22	-18
	6	2.5	0.2	0.2	38	4.2	10	-18
Nanocrystalline w_c=41, h_c=120, A=36, B=30, w_0=76, l_0=64, w_1=84, l_1=72	1	2.5	4	4	105.6	7.2	9	54
	2	2.5	0.2	0.2	81.8	7.2	7	54
	3	2.5	21.8	21.8	109.4	5.3	28	-18
	4	2.5	0.2	0.2	78	5.3	20	-18

The dimensions are in mm and the currents are in A.
g_{in} represents the layer-to-layer gaps inside the core window and g_{out} represents the layer-to-layer gaps outside the core window.

ACKNOWLEDGMENT

The authors would like to thank Dr. Amin Bahmani for his contribution in designing the transformers.

REFERENCES

[1] F. Blaabjerg, M. Liserre, and K. Ma, "Power electronics converters for wind turbine systems," *IEEE Trans. Ind. Appl.*, vol. 48, no. 2, pp. 708–719, Mar./Apr. 2012.

[2] M. Forouzesh, Y. P. Siwakoti, S. A. Gorji, F. Blaabjerg, and B. Lehman, "Step-up DC–DC converters: A comprehensive review of voltage-boosting techniques, topologies, and applications," *IEEE Trans. Power Electron.*, vol. 32, no. 12, pp. 9143–9178, Dec. 2017.

[3] M. A. Bahmani, T. Thiringer, and M. Kharezy, "Design methodology and optimization of a medium-frequency transformer for high-power DC–DC applications," *IEEE Trans. Ind. Appl.*, vol. 52, no. 5, pp. 4225–4233, Oct. 2016.

[4] M. A. Bahmani and T. Thiringer, "Accurate evaluation of leakage inductance in high-frequency transformers using an improved frequency-dependent expression," *IEEE Trans. Power Electron.*, vol. 30, no. 10, pp. 5738–5745, Oct. 2015.

[5] M. Kharezy, M. Eslamian, and T. Thiringer, "Insulation design of a medium frequency power transformer for a cost-effective series high voltage DC collection network of an offshore wind farm," in *Proc. 21st Int. Symp. High Voltage Eng. (ISH)*, Budapest, Hungary, 2019, pp. 1406–1417.

[6] M. Kharezy, H. R. Mirzaei, Y. Serdyuk, T. Thiringer, and M. Eslamian, "A novel oil-immersed medium frequency transformer for offshore HVDC wind farms," *IEEE Trans. Power Del.*, early access, Nov. 3, 2020, doi: 10.1109/TPWRD.2020.3035718.

[7] B. Chen, X. Liang, and N. Wan, "Design methodology for inductor-integrated litz-wired high-power medium-frequency transformer with the nanocrystalline core material for isolated DC-link stage of solid-state transformer," *IEEE Trans. Power Electron.*, vol. 35, no. 11, pp. 11557–11573, Nov. 2020.

[8] Z. Ouyang, J. Zhang, and W. G. Hurley, "Calculation of leakage inductance for high-frequency transformers," *IEEE Trans. Power Electron.*, vol. 30, no. 10, pp. 5769–5775, Oct. 2015.
[9] K. Zhang, W. Chen, X. Cao, P. Pan, S. W. Azeem, G. Qiao, and F. Deng, "Accurate calculation and sensitivity analysis of leakage inductance of high-frequency transformer with Litz wire winding," *IEEE Trans. Power Electron.*, vol. 35, no. 4, pp. 3951–3962, Apr. 2020.
[10] A. Fouineau, M.-A. Raulet, B. Lefebvre, N. Burais, and F. Sixdenier, "Semi-analytical methods for calculation of leakage inductance and frequency-dependent resistance of windings in transformers," *IEEE Trans. Magn.*, vol. 54, no. 10, pp. 1–10, Oct. 2018.
[11] P. L. Dowell, "Effects of eddy currents in transformer windings," *Proc. Inst. Electr. Eng.*, vol. 113, no. 8, pp. 1387–1394, Aug. 1966.
[12] J. A. Ferreira, "Improved analytical modeling of conductive losses in magnetic components," *IEEE Trans. Power Electron.*, vol. 9, no. 1, pp. 127–131, Jan. 1994.
[13] M. A. Bahmani, T. Thiringer, A. Rabiei, and T. Abdulahovic, "Comparative study of a multi-MW high-power density DC transformer with an optimized high-frequency magnetics in all-DC offshore wind farm," *IEEE Trans. Power Del.*, vol. 31, no. 2, pp. 857–866, Apr. 2016.
[14] M. Mogorovic and D. Dujic, "Sensitivity analysis of medium-frequency transformer designs for solid-state transformers," *IEEE Trans. Power Electron.*, vol. 34, no. 9, pp. 8356–8367, Sep. 2019.
[15] G. Ortiz, J. Biela, and J. W. Kolar, "Optimized design of medium frequency transformers with high isolation requirements," in *Proc. 36th Annu. Conf. IEEE Ind. Electron. Soc. (IECON)*, Glendale, AZ, USA, Nov. 2010, pp. 631–638.
[16] S. V. Kulkarni, S. A. Khaparde, *Transformer Engineering: Design, Technology and Diagnostics*. New York, NY, USA: Taylor & Francis, 2013.
[17] K. Karsai, D. Kerényi, and L. Kiss, *Large Power Transformers*. Amsterdam, The Netherlands: Elsevier, 1987.
[18] X. Guo, C. Li, Z. Zheng, and Y. Li, "A general analytical model and optimization for leakage inductances of medium-frequency transformers," *IEEE J. Emerg. Sel. Topics Power Electron.*, early access, Feb. 21, 2021, doi: 10.1109/JESTPE.2021.3062019.
[19] M. Lambert, F. Sirois, M. Martinez-Duro, and J. Mahseredjian, "Analytical calculation of leakage inductance for low-frequency transformer modeling," *IEEE Trans. Power Del.*, vol. 28, no. 1, pp. 507–515, Jan. 2013.
[20] X. Margueron, A. Besri, P.-O. Jeannin, J.-P. Keradec, and G. Parent, "Complete analytical calculation of static leakage parameters: A step toward HF transformer optimization," *IEEE Trans. Ind. Appl.*, vol. 46, no. 3, pp. 1055–1063, Mar. 2010.
[21] I. Hernandez, F. de Leon, and P. Gomez, "Design formulas for the leakage inductance of toroidal distribution transformers," *IEEE Trans. Power Del.*, vol. 26, no. 4, pp. 2197–2204, Oct. 2011.
[22] E. Roth, "Étude analytique du champ de fuites des transformateurs et des efforts mécaniques exercés sur les enroulements," *Revue générale de l'électricité*, vol. 23, pp. 773–787, May 1928.
[23] A. Boyajian, "Leakage reactance of irregular distributions of transformer windings by the method of double Fourier series [includes discussion]," *Trans. Amer. Inst. Electr. Eng. III, Power App. Syst.*, vol. 73, no. 2, pp. 1078–1086, Jan. 1954.
[24] E. Billig, "The calculation of the magnetic field of rectangular conductors in a closed slot, and its application to the reactance of transformer windings," *Proc. IEE IV, Inst. Monographs*, vol. 98, no. 1, pp. 55–64, Oct. 1951, doi: 10.1049/pi-4.1951.0007.
[25] A. L. Morris, "The influence of various factors upon the leakage reactance of transformers," *J. Inst. Electr. Eng.*, vol. 86, no. 521, pp. 485–495, May 1940, doi: 10.1049/jiee-1.1940.0068.
[26] P. Hammond, "Roth's method for the solution of boundary-value problems in electrical engineering," *Proc. Inst. Elect. Eng.*, vol. 114, no. 12, pp. 1969–1976, Dec. 1967.
[27] R. Schlesinger and J. Biela, "Comparison of analytical models of transformer leakage inductance: Accuracy versus computational effort," *IEEE Trans. Power Electron.*, vol. 36, no. 1, pp. 146–156, Jan. 2021, doi: 10.1109/TPEL.2020.3001056.
[28] O. Andersen, "Transformer leakage flux program based on the finite element method," *IEEE Trans. Power App. Syst.*, vol. PAS-92, no. 2, pp. 682–689, Mar. 1973, doi: 10.1109/TPAS.1973.293773.
[29] P. Silvester and A. Konrad, "Analysis of transformer leakage phenomena by high-order finite elements," *IEEE Trans. Power App. Syst.*, vol. PAS-92, no. 6, pp. 1843–1855, Nov. 1973, doi: 10.1109/TPAS.1973.293564.
[30] M. Nazmunnahar, S. Simizu, P. R. Ohodnicki, S. Bhattacharya, and M. E. McHenry, "Finite-element analysis modeling of high-frequency single-phase transformers enabled by metal amorphous nanocomposites and calculation of leakage inductance for different winding topologies," *IEEE Trans. Magn.*, vol. 55, no. 7, pp. 1–11, Jul. 2019.
[31] W. G. Hurley and W. H. Wölfle, *Transformers and Inductors for Power Electronics*. Hoboken, NJ, USA: Wiley, 2013.
[32] M. Eslamian, M. Kharezy, and T. Thiringer, "Calculation of the leakage inductance of medium frequency transformers with rectangular-shaped windings using an accurate analytical method," in *Proc. 21st Eur. Conf. Power Electron. Appl. (EPE ECCE Eur.)*, Genova, Italy, Sep. 2019, pp. 3–5.
[33] M. Kharezy, "Constructional design, manufacturing and evaluation of high-power density medium frequency transformer prototypes," Chalmers Univ. Technol., Gothenburg, Sweden, Tech. Rep. 211818, Dec. 2014. [Online]. Available: http://publications.lib.chalmers.se/records/fulltext/211818/211818.pdf
[34] M. K. Kazimierczuk, *High-Frequency Magnetic Components*. Hoboken, NJ, USA: Wiley, 2014.

MORTEZA ESLAMIAN received the M.Sc. and Ph.D. degrees in electrical engineering from the Amirkabir University of Technology, Tehran, Iran, in 2009 and 2014, respectively. Since 2014, he has been with the Department of Electrical Engineering, University of Zanjan, Iran, where he is currently working as an Assistant Professor. He is also a member of Iran Transformer Research Institute (ITRI), from 2005, where he has directed several industrial projects in the area of power transformers. His research interests include power and special transformers, power system transients, high voltage and electrical insulation, and electrical installation and distribution systems.

MOHAMMAD KHAREZY (Member, IEEE) received the B.Sc. degree in electrical engineering from the University of Tabriz, in 1991, and the M.Sc. and Licentiate degrees in electrical engineering from the Chalmers University of Technology, Sweden, in 2014 and 2020, respectively, where he is currently pursuing the Ph.D. degree in electrical power industrial. He worked for 18 years in the field of power transformers. Since 2011, he has been working as a High Voltage Researcher with the Research Institutes of Sweden (RISE). He has contributed to several international scientific articles. His research interests include medium frequency power transformers and high voltage insulation, and measurement and testing technologies. He is a member of Cigré.

TORBJÖRN THIRINGER (Senior Member, IEEE) received the M.Sc. and Ph.D. degrees from the Chalmers University of Technology, Göteborg, Sweden, in 1989 and 1996, respectively. He is currently working as a Professor of applied power electronics with the Chalmers University of Technology. His research interests include modeling, control, and grid integration of wind energy converters into power grids, battery technology from detailed cell modeling to system aspects, and power electronics and drives for other types of applications, such as electrified vehicles, buildings, and industrial applications.